Hindawi
Mobile Information Systems
Volume 2022, Article ID 8720801, 11 pages
https://doi.org/10.1155/2022/8720801

Research Article

Collaborative Optimization Model of Highway Network with Tourism Resources as the Target Node

Wei Niu

International Business School, Global Institute of Software Technology, Suzhou 215163, China

Correspondence should be addressed to Wei Niu; wniu@gist.edu.cn

Received 15 April 2022; Revised 8 June 2022; Accepted 9 July 2022; Published 21 August 2022

Academic Editor: Yajuan Tang

In order to improve the collaborative optimization effect of tourism resources and highway network, this paper combines deep learning algorithm to construct a collaborative optimization model of tourism resources and highway network, and adopts an algorithm based on continuous convex approximation. By iterating the optimal solution obtained each time, a high-quality approximate beamforming matrix and artificial noise covariance matrix can finally be obtained, which eliminates the problem that the traditional algorithm cannot solve the noise. Moreover, this paper introduces artificial noise to prove that the rank relaxation is compact by considering the corresponding minimization power problem. The simulation results show that the proposed scheme and approximation algorithm can obtain better system security and speed than the existing literature, and there are certain improvements compared with the traditional method, so the effectiveness of the method in this paper is verified by simulation experiments.

1. Introduction

The research on the interaction between the transportation system and the tourism system has always been a hot topic in the discussion of spatial geography. The continuous development of the expressway network, which is the key to the transportation system, has an increasingly obvious impact on the development of tourism resources, and the development of the tourism industry in turn promotes or restricts the extension of the expressway network.

Through the analysis of the structural characteristics of the regional passenger transportation network, we locate the roles and functions of each tourism node in the passenger flow network and transportation network, and find out and identify potential traffic improvement nodes and tourism investment nodes. The operation effect of the entire regional highway network can be optimized, and the total social investment benefit can be maximized. This provides new ideas for highway planning and a theoretical basis for regional highway network planning decision-makers, to effectively save the travel time and travel costs of road travelers, improve travel satisfaction, and further increase the revisit rate of big tourist travelers.

The main contributions of this paper are as follows: in the previous provincial expressway network planning, only the connectivity of major cities was generally considered, and the connectivity of tourist attractions was not included. With the continuous development of tourism and the improvement of the service demand of tourist attractions, the planning of high-speed tourist highways will become inevitable. In this paper, combined with deep learning, the tourism resources and the road network collaborative optimization model are linked, and it is hoped that the planned road network tourism resources' demand will increase the most. From the point of view of network users (travelers), each user wishes to travel with the least amount of time or expense.

In this paper, through this optimization method, this paper optimizes the allocation of tourism resources; at the same time, improves the operation efficiency of the highway network; and provides a strong support for the integration, development, and utilization of regional system resources.

2. Related Work

The research on tourism spatial structure is an extension of the research theory of regional spatial structure. The research

on regional spatial structure accompanies the time course from the agricultural era to the industrial era. Foreign scholars have put forward the spatial structure theories divided by economic industries, such as agricultural regional theory and industrial location theory [1]. The regional spatial evolution structure of different grades of central places with decreasing scale from top to bottom under the constraints of different factors is proposed, that is, the principle of central places [2]. The study puts forward the growth pole theory, which holds that economic growth first occurs on the growth pole, and then spreads to the surrounding areas in different ways [3]. Taking increasing returns and monopolistic competition as analytical tools for the study of the regional spatial economy, he proposes the "center-periphery" theory [4], arguing that the spatial distribution pattern of economic activities will eventually reach equilibrium under the influence of agglomeration and dispersion.

The research system of tourism geography is summarized [5]. It is proposed that the places where tourists gather, such as hotels and restaurants, can be used as a tourist bubble, which can be divided into the core area and the peripheral area, and tourism-influenced activities are mainly concentrated in the core area [6]. By analyzing the tourism spatial characteristics of the most important international tourism regions in South Africa, it is believed that tourism activities are mainly concentrated in a few regions and are concentrated [7]. The study found that the tourism fringe area is an important part of tourism development [8]. The "core-periphery" model of tourism space has been applied in many cases, and through the comparative study of the spatial distribution of the tourism industry, it is found that the tourism industry tends to be concentrated in the central cities [9].

The study found that destination transportation cost and destination living cost are important influencing factors of tourism behavior [9]. The study analyzed that high-speed transportation infrastructure such as highways and high-speed railways (high-speed rail) can promote long-distance travel for tourists [10].

The study believes that the lack of accessibility in India caused by aviation policy is an important factor hindering the development of tourism in India [11]. In terms of analysis methods for measuring the impact of transportation infrastructure on space, the accessibility analysis model is often used to measure the change in regional spatial pattern, and measurement indicators such as distance and weighted time are used to analyze the impact of transportation accessibility on the change in regional pattern [12].

Foreign research on road network optimization problems is mainly reflected in the research on network design problems (NDP, network design problem). According to the different conditions of the road network optimization, the decision variables can be divided into continuous and discrete. For the improvement of road capacity, discrete variables correspond to the problem of new roads [13]. The type of decision variables in network design problems determines the type of optimization model to be constructed, so network optimization problems can be divided into three categories: continuous, discrete, and mixed according to the different types of variables [14]. Among them, the hybrid optimization design problem takes into account the problems of new road sections and reconstruction of existing road sections, which is consistent with the idea of road network optimization in practical engineering. However, since the hybrid problem involves two types of decision variables, the solution of its optimization model method design is the most difficult of the three types of models [15]. Road linearity, geographic conditions, etc. are the constraints [16]. We combined the discrete network design with road route selection optimization and established a two-layer optimization model for continuous route layout. From the perspective of macro planners, the model can optimize road network corridor selection and route layout at the same time [14]. A double-layer planning model for highway network lines is constructed, which takes into account factors such as expressway operation, earthworks, and line collinearity [17]. On the basis of considering travel demand, construction cost, and related soft factors, an optimization model of highway corridor layout is established. A variety of heuristic algorithms are used to solve the model, and it is found that the improved simulated annealing algorithm can better deal with the local minimum problem under low traffic demand [18].

3. Network Collaborative Optimization Model

The realization of the highway initial path generation based on deep reinforcement learning can solve the problem that the manually selected route cannot approach the optimal and provide the basis for the generation of the highway route path based on the deep reinforcement learning. It can promote the simulation of the model in this paper.

As shown in Figure 1, it consists of a source node, a legitimate destination node, K relay nodes, and M eavesdropping nodes. The source node tries to send confidential information to the destination node in the presence of M listening nodes. It is assumed that there is no direct link between the destination node and the source node, and all the information transfer between them needs to be completed by the relay node. Since there is information leakage in the two-hop link, all relay nodes are divided into two. The K_R nodes used to transmit confidential information are called cooperative relays, and the K_J nodes used to generate interference signals to weaken the listening nodes are called interference relays, where $K_R + K_J = K$.

Here, we consider the scenario where eavesdropping nodes are also system users, but they do not have the right to receive services provided by the current source, such as pay TV services. Therefore, it is assumed that the global CSI (including the CSI of the eavesdropping node) is known, and all channels experience slow fading with flat frequency. Among them, the vector $\mathbf{f}, \mathbf{g}_R \in \mathbb{C}^{K_R}$ represents the channel from the source to the cooperative relay, and from the cooperative relay to the destination node, respectively. The vector $\mathbf{g}_J, \mathbf{h}_l \in \mathbb{C}^{K_J}$ represents the channel from the interfering relay to the destination node, to the l-th eavesdropping node, and there is $\mathbf{H}_J \triangleq [\mathbf{h}_1, \ldots, \mathbf{h}_M]$.

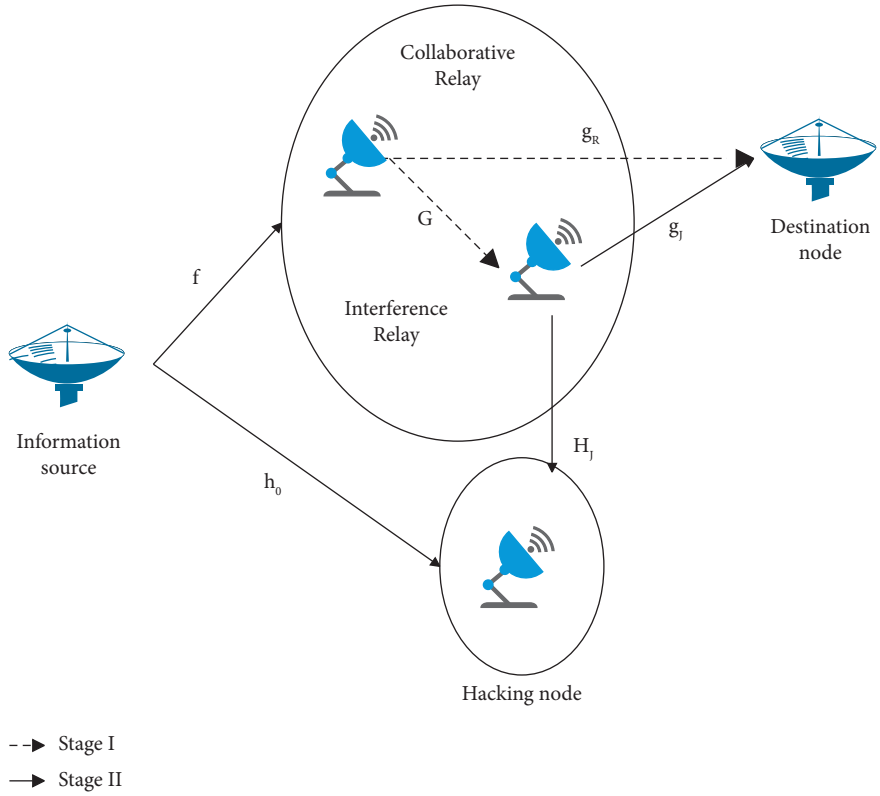

Figure 1: One-way AF relay network with multiple eavesdroppers.

In the traditional secure relay network, the cooperative beamforming and cooperative interference techniques complete information transfer and signal interference within two time slots. In the proposed new transmission scheme, these two functions will be extended to three slots, so we will describe the transmission process with a three-slot transfer model.

In the first time slot, that is, the broadcast stage in the relay two-hop, the source broadcasts a unit energy signal s to all cooperative relays, and this signal will be monitored by the eavesdropping node at the same time. In order to interfere with the eavesdropping node listening to confidential information, the interfering relay generates a set of artificial noise locally and transmits the interference signal $\mathbf{t}_J$. In this time slot, the signal containing the useful signal s received by the cooperative relay and eavesdropping node can be written in the following form, where the superscript indicates the serial number of the time slot in question.

$$\mathbf{y}_R = \sqrt{P_S}\mathbf{f}s + \mathbf{n}_R, \tag{1}$$

$$y_{E,l}^{(1)} = \sqrt{P_S}h_{0,l}s + h_l^T t_J + n_{E,l}^{(1)}, \quad \forall l \in M, \tag{2}$$

In the above formula, for simple processing, the above artificial noise is designed in the null space of all cooperative relays and destination nodes, so as not to bring additional interference to them. If the interfering relay works in the receiving mode, the information security of this time slot completely depends on the cooperative relay. Similarly, using the idea of null space to design the beamforming weight vector at the cooperative relay can ensure that no information is leaked to the eavesdropping node.

In the second time slot, that is, the relay stage in the relay two-hop, the cooperative relay adopts the AF-based cooperative beamforming strategy to forward the information of the source to the destination node. The received signal about s involved in this time slot is only at the interfering node and the destination node.

$$y_J = G^T t_R + n_J, \tag{3}$$

$$y_D^{(2)} = \mathbf{g}_R^T \mathbf{t}_R + n_D^{(2)}, \tag{4}$$

The introduction of the third time slot is to allow the interfering relay to complete the transfer of confidential information s to the destination node. The difference is that the source emits the next useful signal with unit energy. The signal $\mathbf{t}_J$ at the interfering node is no longer only composed of artificial noise. It can be seen that all copies of the signal s can be received by the destination node only after the transmission of the above three time slots is completed.

As mentioned earlier, the null-space design of artificial noise completely eliminates its influence on cooperative relays and destination nodes. Similarly, the useful signal part $\mathrm{D}(\mathrm{y}_J)\mathbf{v}$ in $\mathbf{t}_J$ is designed in the null space of eavesdropping nodes and cooperative relays. In this way, on the one hand, information leakage is prevented, and on the other hand, the mutual interference between the two groups of relay nodes is

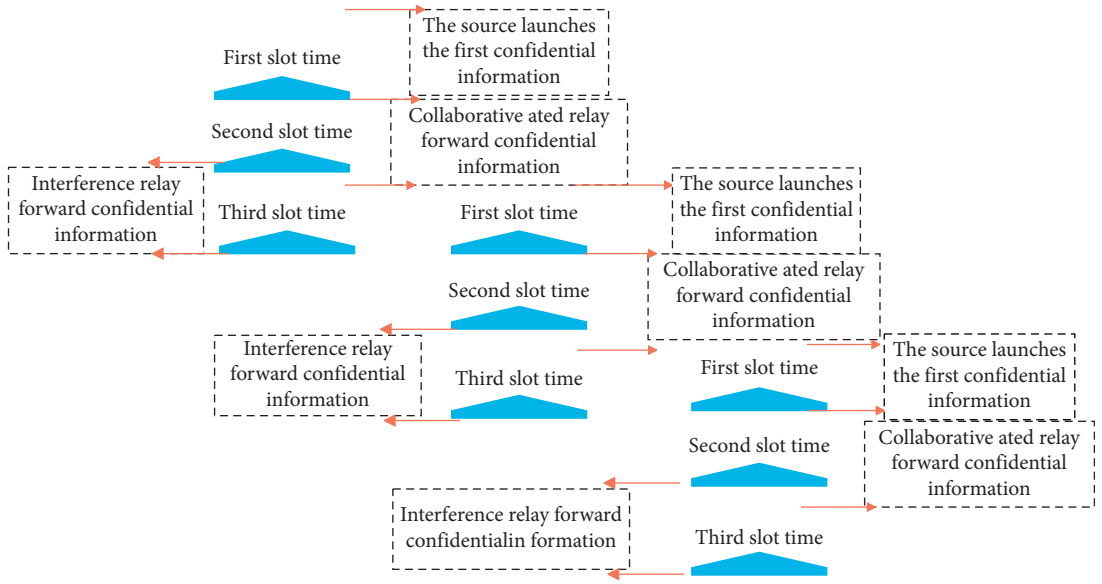

Figure 2: Time slot diagram.

avoided. Since only the reception containing the copy of the s signal is concerned, in the third time slot, there is only a received signal about s at the destination node.

$$y_D^{(3)} = \mathbf{g}_J^T \mathbf{t}_J + n_D^{(3)} = \sqrt{P_S}\mathbf{w}^T \mathbf{D}(\mathbf{f})\mathbf{G}\ \mathbf{D}\left(\mathbf{g}_J\right)\mathbf{v}s + \mathbf{n}_R^T \mathbf{D}(\mathbf{w})\mathbf{G}\ \mathbf{D}\left(\mathbf{g}_J\right)\mathbf{v} + \mathbf{n}_J^T \mathbf{D}\left(\mathbf{g}_J\right)\mathbf{v} + n_D^{(3)} \tag{5}$$

For the confidential signal generated by the next source, its transmission mode is the same as s, which can be described by the above three time slots. It should be noted that t_J will always remain in the form of a mixed signal, as shown in equation (4). In the expression (2) of the signal received by the corresponding eavesdropping node, $\mathbf{h}_l^T \mathbf{t}_J$ needs to be changed to $\mathbf{h}_l^T \mathbf{n}_a$. In the proposed transmission model, a signal is transmitted across three time slots. However, it can be easily analyzed that the broadcast stages of the two connected signals overlap, as shown in Figure 2.

Therefore, the transmission efficiency of this scheme is $N/(2N+1)$, where N is the frame length. When the value of N is large, the transmission efficiency will tend to 1/2, which is the same as the traditional cooperative relay system. In addition, if the useful signal part in $\mathbf{t}_J$ is ignored, the scheme can easily degenerate into a situation that the traditional interference relay only sends artificial noise. Below, the above null space constraints on $\mathbf{w}, \mathbf{v}$, and $\mathbf{n}_a$ are summarized as follows.

According to the above constraints of null space, in order to ensure sufficient spatial degrees of freedom, the selection of the number of cooperative relays, interfering relays, and eavesdropping nodes needs to satisfy two conditions: $K_R \geq M+1$ and $K_J \geq K_R + M + 1$. When the vector $\mathrm{z}_0, \mathrm{z}_1$ and the covariance matrix Σ are given, according to the signal model in formulas (2), (4), and (5), the received signal-to-noise ratio at the destination node and the eavesdropping node can be calculated as follows:

$$\gamma_{E,l}^{(1)} = \frac{P_S |h_{0,l}|^2}{\mathrm{Tr}\left(\mathbf{H}_l \boldsymbol{\Sigma}\right) + 1}, \forall l, \tag{6}$$

$$\gamma_D^{(2)} = \frac{\mathbf{z}_0^H \mathbf{B}\mathbf{z}_0}{\mathbf{z}_0^H \mathbf{Q}_R \mathbf{z}_0 + 1}, \tag{7}$$

$$\gamma_D^{(3)} = \frac{\mathbf{z}_1^H \mathbf{A}_2^H \mathbf{U}_0^* \mathbf{z}_0^* \mathbf{z}_0^T \mathbf{U}_0^T \mathbf{A}_2 \mathbf{z}_1}{\mathbf{z}_1^H \mathbf{A}_1^H \mathbf{D}\left(\mathbf{U}_0^* \mathbf{z}_0^* \mathbf{z}_0^T \mathbf{U}_0^T\right)\mathbf{A}_1 \mathbf{z}_1 + \mathbf{z}_1^H \mathbf{Q}_J \mathbf{z}_1 + 1}. \tag{8}$$

Therefore, the achievable safe rate can be defined as the following form:

$$R_s(\mathbf{z}_0, \mathbf{z}_1, \boldsymbol{\Sigma}) = \frac{1}{2}\min_{l \in \mathcal{M}} \left\{\log\left(1 + \gamma_D^{(2)} + \gamma_D^{(3)}\right) - \log\left(1 + \gamma_{E,l}^{(1)}\right)\right\}. \tag{9}$$

In the formula, $\log(\cdot)$ represents the logarithmic function of base two, and the coefficient 1/2 is the approximate relay transmission efficiency when N is large. It should be noted that $R_s(\mathbf{z}_0, \mathbf{z}_1, \Sigma)$ represents a certain transmission rate at which the destination node can decode the confidential information but the eavesdropping node cannot.

This paper focuses on a joint beamforming and artificial noise design scheme based on safety rate maximization. First, the constraints of each relay's own power are given, which can be obtained as follows:

$$\begin{aligned} \mathbf{E}\left\{\left|y_{R,i} w_i\right|^2\right\} &= \mathbf{e}_{R,i}^T \mathbf{C}_R \mathbf{U}_0 \mathbf{z}_0 \mathbf{z}_0^H \mathbf{U}_0^H \mathbf{e}_{R,i} \leq P_{1,i}, \quad \forall i \\ \mathbf{E}\left\{\left|y_{J,k} v_k + n_{a,k}\right|^2\right\} &= \mathbf{e}_{J,k}^T \left(\mathbf{C}_J \mathbf{U}_1 \mathbf{z}_1 \mathbf{z}_1^H \mathbf{U}_1^H + \mathbf{U}_2 \boldsymbol{\Sigma} \mathbf{U}_2^H\right)\mathbf{e}_{J,k} \leq P_{2,k}, \quad \forall k \end{aligned} \tag{10}$$

In the formula, $\mathbf{e}_{R,i} \in \mathbb{C}^{K_R}$ represents the unit vector whose ith element is one, $\mathbf{e}_{J,k} \in \mathbb{C}^{K_J}$ represents the unit vector whose kth element is one, and $\mathbf{I}_{K_R}$ represents the unit matrix whose size is K_R. Meanwhile, $P_{1,i}$ and $P_{2,k}$ denote the

own power budgets of the ith cooperative relay and the kth interfering relay, respectively.

The goal of this scheme is to maximize the safe rate under the power constraints of each cooperative relay and interfering relay. The optimization problem after ignoring the constant \$1/2\$ can be expressed as follows:

$$\begin{aligned}&\max_{\mathbf{z}_0,\mathbf{z}_1,\boldsymbol{\Sigma}} \min_{l\in\mathscr{M}}\left\{\log\left(1+\gamma_D^{(2)}+\gamma_D^{(3)}\right)-\log\left(1+\gamma_{E,l}^{(1)}\right)\right\}\\ &\text{s.t.}\quad \mathbf{e}_{J,k}^T\left(\mathbf{C}_J\mathbf{U}_1\mathbf{z}_1\mathbf{z}_1^H\mathbf{U}_1^H+\mathbf{U}_2\boldsymbol{\Sigma}\mathbf{U}_2^H\right)\mathbf{e}_{J,k}\le P_{2,k},\ \forall k\\ &\quad \mathbf{e}_{R,i}^T\mathbf{C}_R\mathbf{U}_0\mathbf{z}_0\mathbf{z}_0^H\mathbf{U}_0^H\mathbf{e}_{R,i}\le P_{1,i},\ \forall i\end{aligned}\tag{11}$$

Problem (11) is nonconvex. It is difficult to solve. In order to simplify the problem, problem (11) is decomposed into two subproblems. First, z_1 and Σ are not considered, and z_0 is only optimized with the goal of maximizing $\gamma_D^{(2)}$. The second subproblem utilizes the obtained $\mathrm{z}_{0,\mathrm{opt}}$ to optimize z_1 and Σ according to the corresponding criteria. Such a decomposition undoubtedly results in a loss of safe rate performance, since z_0, z_1 and Σ cannot be jointly optimized. However, the subsequent simulation results prove that the above suboptimal solution can still achieve a good safe rate. The first subproblem can be expressed as follows:

$$\begin{aligned}&\min_{\mathbf{z}_0}\frac{\mathbf{z}_0^H\mathbf{Q}_R\mathbf{z}_0+1}{\mathbf{z}_0^H\mathbf{B}\mathbf{z}_0},\\ &\text{s.t. }\mathbf{e}_{R,i}^T\mathbf{C}_R\mathbf{U}_0\mathbf{z}_0\mathbf{z}_0^H\mathbf{U}_0^H\mathbf{e}_{R,i}\le P_{1,i},\ \forall i,\end{aligned}\tag{12}$$

In order to solve the above problems effectively, problem (12) is first relaxed into a convex semidefinite program (SDP) with the help of semidefinite relaxation (SDR) and Charnes–Cooper transformation. By defining $\mathbf{Z}_0 \triangleq \xi\mathbf{z}_0\mathbf{z}_0^H$, and there is $\xi > 0$, the semidefinite relaxation problem of problem (12) can be obtained as follows:

$$\begin{aligned}&\min_{\mathbf{Z}_0,\xi}\mathrm{Tr}\left(\mathbf{Q}_R\mathbf{Z}_0\right)+\xi\\ &\text{s.t.}\mathrm{Tr}\left(\mathbf{B}\mathbf{Z}_0\right)=1\\ &\mathrm{Tr}\left(\mathbf{U}_0^H\mathbf{e}_{R,i}\mathbf{e}_{R,i}^T\mathbf{C}_R\mathbf{U}_0\mathbf{Z}_0\right)\le\xi P_{1,i},\ \forall i\\ &\mathbf{Z}_0\succcurlyeq 0,\ \xi\ge 0.\end{aligned}\tag{13}$$

Problem (13) is a convex problem, so it can be solved directly by the toolkit SeDuMi or CVX based on interior point methods. Since problem (12) is relaxed into the form of problem (13), a semidefinite relaxation method is adopted, and the rank-one constraint of $\mathbf{Z}_0$'s nonconvexity is removed, so it seems that the two problems are not equivalent. However, through the following theorem, we will prove that the abovementioned rank relaxation is compact, that is, the only optimal $\mathbf{z}_{0,\mathrm{opt}}$ can be obtained from the matrix $\mathbf{Z}_0$.

Theorem 1. *If it is assumed that problem (13) is feasible, and $(\mathbf{Z}_{0,opt}, \xi_{opt})$ is the optimal solution to problem (13), the rank of $\mathbf{Z}_{0,opt}$ must be equal to one.*

Proof. It can be seen that all problems in problem (13) are linear constraints. If $\mathbf{Z}_{0,\mathrm{opt}}$ is the optimal solution of problem (13), the optimal solution of $\mathbf{Z}_{0,\mathrm{opt}}$ and its dual problem satisfies the KKT condition. The KKT conditions related to the proof are listed as follows:

$$\mathbf{Y}=\mathbf{Q}_R-\mu_0\mathbf{B}+\sum_{i=1}^{K_R}\mu_i\mathbf{U}_0^H\mathbf{e}_{R,i}\mathbf{e}_{R,i}^T\mathbf{C}_R\mathbf{U}_0,\tag{14}$$

$$\mathbf{Y}\mathbf{Z}_{0,\mathrm{opt}}=0,\tag{15}$$

$$\mathbf{Y}\succcurlyeq 0,\ \mathbf{Z}_{0,\mathrm{opt}}\succcurlyeq 0,\ \mu_i\ge 0,\ \forall i.\tag{16}$$

In the formula, μ_0 and $\mathbf{Y}$ are the optimal dual variables corresponding to the equation constraints and $\mathbf{Z}_0\succcurlyeq 0$ constraints in problem (13), respectively. μ_i is a dual variable corresponding to each node's own power constraint. Problem (14) is substituted into problem (15), and we can get the following:

$$\mu_0\mathbf{B}\mathbf{Z}_{0,\mathrm{opt}}=\mathbf{U}_0^H\left(\mathbf{D}^H(\mathbf{g}_R)\mathbf{D}(\mathbf{g}_R)+\sum_{i=1}^{K_R}\mu_i\mathbf{e}_{R,i}\mathbf{e}_{R,i}^T\mathbf{C}_R\right)\mathbf{U}_0\mathbf{Z}_{0,\mathrm{opt}}\tag{17}$$

Among them, $\mathbf{D}^H(\mathbf{g}_R)\mathbf{D}(\mathbf{g}_R)+\sum_{i=1}^{K_R}\mu_i\mathbf{e}_{R,i}\mathbf{e}_{R,i}^T\mathbf{C}_R\succ 0.$ is a full rank matrix. Therefore, the following conclusions can be drawn as follows:

$$\begin{aligned}rank\left(\mathbf{Z}_{0,\mathrm{opt}}\right)&=rank\Big(\mathbf{U}_0^H\Big(\mathbf{D}^H(\mathbf{g}_R)\mathbf{D}(\mathbf{g}_R)\\ &\quad+\sum_{i=1}^{K_R}\mu_i\mathbf{e}_{R,i}\mathbf{e}_{R,i}^T\mathbf{C}_R\Big)\mathbf{U}_0\mathbf{Z}_{0,\mathrm{opt}}\Big)\\ &=rank\left(\mu_0\mathbf{B}\mathbf{Z}_{0,\mathrm{opt}}\right)\le rank(\mathbf{B})=1\end{aligned}\tag{18}$$

Obviously, $\mathrm{rank}(\mathbf{Z}_{0,\mathrm{opt}})=0$ is impossible because $\mathbf{Z}_{0,\mathrm{opt}}=0$ is infeasible for the equality constraints in problem (15). Therefore, $rank(\mathbf{Z}_{0,\mathrm{opt}})=1$ must hold.

According to Theorem 1, we can simply extract the optimal solution $\mathbf{z}_{0,\mathrm{opt}}$ of problem (12) from $\mathbf{Z}_{0,\mathrm{opt}}$ by eigenvalue decomposition. On the basis of obtaining $\mathbf{z}_{0,\mathrm{opt}}$, the corresponding $\gamma_{D,\mathrm{opt}}^2$ can be calculated by substituting it into formula (6). After the solution to the first subproblem is known, the results that have been obtained are used to turn to the second subproblem, which is shown below as follows:

$$\begin{aligned}&\max_{\mathbf{z}_1,00}\min_{l\in\mathscr{M}}\left\{\log\left(1+\gamma_{D,\,\mathrm{opt}}^{(2)}+\gamma_D^{(3)}\right)-\log\left(1+\gamma_{E,l}^{(1)}\right)\right\}\\ &\text{s.t. }\mathbf{e}_{J,k}^T\left(\mathbf{C}_J\mathbf{U}_1\mathbf{z}_1\mathbf{z}_1^H\mathbf{U}_1^H+\mathbf{U}_2\boldsymbol{\Sigma}\mathbf{U}_2^H\right)\mathbf{e}_{J,k}\le P_{2,k},\ \forall k.\end{aligned}\tag{19}$$

It can be seen that the objective function of problem (19) is in the form of the subtraction of two concave functions, and it is very difficult to solve it directly. In order to effectively solve the above problem, a slack variable τ is introduced. It aims to solve the original problem into an optimization problem with a two-layer structure. First, the inner layer problem is solved. For any feasible τ, the inner layer problem can be expressed as follows:

$$\max_{\mathbf{z}_1,\Sigma\succcurlyeq 0}\left\{\log\left(1+\gamma_{D,\mathrm{opt}}^{(2)}+\gamma_D^{(3)}\right)-\log\left(\frac{1}{\tau}\right)\right\}$$
$$\text{s.t.}\log\left(1+\gamma_{E,l}^{(1)}\right)\le \log\left(\frac{1}{\tau}\right),\forall l \tag{20}$$
$$\mathbf{e}_{J,k}^T\left(\mathbf{C}_J\mathbf{U}_1\mathbf{z}_1\mathbf{z}_1^H\mathbf{U}_1^H+\mathbf{U}_2\Sigma\mathbf{U}_2^H\right)\mathbf{e}_{J,k}\le P_{2,k},\forall k.$$

Since the logarithmic function is monotonically increasing, it can be removed. After the specific expressions of $\gamma_D^{(3)}$ and $\gamma_{E,l}^{(1)}$ are substituted, the following form can be further obtained:

$$\max_{\mathbf{z}_1,\Sigma\succcurlyeq 0}\tau\left(1+\frac{\mathbf{z}_1^H\mathbf{A}_2^H\mathbf{W}_{\mathrm{opt}}^*\mathbf{A}_2\mathbf{z}_1}{\mathbf{z}_1^H\left(\mathbf{A}_1^H\mathbf{D}\left(\mathbf{W}_{\mathrm{opt}}^*\right)\mathbf{A}_1+\mathbf{Q}_J\right)\mathbf{z}_1+1}\right)$$
$$\text{s.t.}\tau\left(\frac{P_S\left|h_{0,l}\right|^2}{\mathrm{Tr}\left(\mathbf{H}_l\Sigma\right)+1}+1\right)\le 1,\forall l \tag{21}$$
$$\mathbf{e}_{J,k}^T\left(\mathbf{C}_J\mathbf{U}_1\mathbf{z}_1\mathbf{z}_1^H\mathbf{U}_1^H+\mathbf{U}_2\Sigma\mathbf{U}_2^H\right)\mathbf{e}_{J,k}\le P_{2,k},\forall k.$$

In the formula, there is $\mathbf{W}_{\mathrm{opt}}^*\triangleq\mathbf{U}_0\mathbf{z}_{0,\mathrm{opt}}\mathbf{z}_{0,\mathrm{opt}}^H\mathbf{U}_0^H$. In the objective function of problem (21), the operation of ignoring $\gamma_{D,\mathrm{opt}}^{(2)}$ does not affect the solution of the entire optimization problem. This is because for any given τ, $\gamma_{D,\mathrm{opt}}^{(2)}$ is a constant. Similar semidefinite relaxation techniques and Charnes–Cooper transformations to the first subproblem are employed. In order to write problem (21) as a convex semidefinite program, first we set the following:

$$\begin{aligned}\mathbf{Z}_1&=\eta\mathbf{z}_1\mathbf{z}_1^H,\\ \mathbf{X}&=\eta\Sigma\end{aligned} \tag{22}$$

At the same time, the original maximization problem is rewritten in the form of minimizing the reciprocal of the original problem as follows:

$$\begin{aligned}&\min_{\mathbf{Z}_1,\mathbf{X},\eta}\mathrm{Tr}\left(\mathbf{A}_1^H\mathbf{D}\left(\mathbf{W}_{\mathrm{opt}}^*\right)\mathbf{A}_1\mathbf{Z}_1+\mathbf{Q}_J\mathbf{Z}_1+\eta\right)\\ &\text{s.t.}\mathrm{Tr}\left(\mathbf{U}_1^H\mathbf{e}_{J,k}\mathbf{e}_{J,k}^T\mathbf{C}_J\mathbf{U}_1\mathbf{Z}_1+\mathbf{U}_2^H\mathbf{e}_{J,k}\mathbf{e}_{J,k}^T\mathbf{U}_2\mathbf{X}\right)\le\eta P_{2,k},\forall k\\ &\tau\left\{\eta\left(1+P_S\left|h_{0,l}\right|^2\right)+\mathrm{Tr}\left(\mathbf{H}_l\mathbf{X}\right)\right\}<\eta+\mathrm{Tr}\left(\mathbf{H}_l\mathbf{X}\right),\forall l\\ &\tau\left\{\mathrm{Tr}\left(\mathbf{A}_1^H\mathbf{D}\left(\mathbf{W}_{\mathrm{opt}}^*\right)\mathbf{A}_1\mathbf{Z}_1+\mathbf{A}_2^H\mathbf{W}_{\mathrm{opt}}^*\mathbf{A}_2\mathbf{Z}_1\right)+\mathrm{Tr}\left(\mathbf{Q}_J\mathbf{Z}_1\right)+\eta\right\}=1\\ &\mathbf{Z}_1\succcurlyeq 0,\mathbf{X}\succcurlyeq 0,\eta\ge 0.\end{aligned} \tag{23}$$

Since problem (23) is convex, its global optimal solution $(\mathbf{Z}_{1,\mathrm{opt}},\mathbf{X}_{\mathrm{opt}},\eta_{\mathrm{opt}})$ can be efficiently solved by SeDuMi or CVX toolkit. The problem now is that if $\mathbf{Z}_{1,\mathrm{opt}}$ is a matrix of rank one, the rank relaxation for the second subproblem is also compact. The optimal $\mathbf{z}_{1,\mathrm{opt}}$ can be directly obtained by eigenvalue decomposition of $\mathbf{Z}_{1,\mathrm{opt}}$. In the following theorem, we will show that the relaxation for $\mathbf{Z}_{1,\mathrm{opt}}$ is also tight.

Theorem 2. *If it is assumed that problem (23) is feasible, and $(\mathbf{Z}_{1,opt},\mathbf{X}_{opt},\eta_{opt})$ is the optimal solution to problem (23), the rank of $\mathbf{Z}_{1,opt}$ must be equal to one.*

Proof. We set $\mathrm{Z}_{1,\mathrm{opt}}\ne 0$ to be the optimal solution to problem (23). Since the constraints in problem (23) are all linear constraints, $\mathbf{Z}_{1,\mathrm{opt}}$ satisfies the KKT condition as follows:

$$\begin{aligned}&-\Psi+(1-\alpha\tau)\left(\mathbf{A}_1^H\mathbf{D}\left(\mathbf{W}_{\mathrm{opt}}^*\right)\mathbf{A}_1+\mathbf{Q}_J\right)\\ &-\alpha\tau\mathbf{A}_2^H\mathbf{W}_{\mathrm{opt}}^*\mathbf{A}_2+\sum_{k=1}^{K_J}\lambda_k\mathbf{U}_1^H\mathbf{e}_{J,k}\mathbf{e}_{J,k}^T\mathbf{C}_J\mathbf{U}_1=0,\end{aligned} \tag{24}$$
$$\Psi\mathbf{Z}_{1,\mathrm{opt}}=0,\Psi\succcurlyeq 0,\mathbf{Z}_{1,\mathrm{opt}}\succcurlyeq 0,\lambda_k\ge 0,\forall k, \tag{25}$$

λ_k corresponds to the power constraints of each cooperating relay and interfering relay. Through the Lagrangian strong duality property, we can simply prove that the value of α is the value of the objective function of problem (23). This means that α must be positive.

$$\begin{aligned}\frac{1}{\left(1+\gamma_{D,\mathrm{opt}}^{(3)}\right)\tau}&=\Phi(\tau)=\alpha,\\ 1-\alpha\tau&=1-\frac{1}{\left(1+\gamma_{D,\mathrm{opt}}^{(3)}\right)}>0.\end{aligned} \tag{26}$$

In the formula, $\Phi(\tau)$ represents the optimal value of problem (23). By substituting problem (24) into $\Psi Z_{1,\mathrm{opt}}=0$, the following formula can be obtained:

$$\begin{aligned}\mathbf{R}\mathbf{Z}_{1,\mathrm{opt}}\triangleq&\left\{(1-\alpha\tau)\left(\mathbf{A}_1^H\mathbf{D}\left(\mathbf{W}_{\mathrm{opt}}^*\right)\mathbf{A}_1+\mathbf{Q}_J\right)\right.\\ &\left.+\sum_{k=1}^{K_J}\lambda_k\mathbf{U}_1^H\mathbf{e}_{J,k}\mathbf{e}_{J,k}^T\mathbf{C}_J\mathbf{U}_1\right\}\mathbf{Z}_{1,\mathrm{opt}}\\ =&\alpha\tau\mathbf{A}_2^H\mathbf{W}_{\mathrm{opt}}^*\mathbf{A}_2\mathbf{Z}_{1,\mathrm{opt}},\end{aligned} \tag{27}$$

It can be seen that $\mathbf{R}$ is a positive definite matrix ($\mathbf{R}>0$), because it is the sum of a positive definite matrix and a positive semidefinite matrix. Then, we can get the following:

$$\begin{aligned}rank\left(\mathbf{Z}_{1,\mathrm{opt}}\right)&=rank\left(\mathbf{R}\mathbf{Z}_{1,\mathrm{opt}}\right)\\ &=\alpha\tau rank\left(\mathbf{A}_2^H\mathbf{W}_{\mathrm{opt}}^*\mathbf{A}_2\mathbf{Z}_{1,\mathrm{opt}}\right)\le rank\left(\mathbf{W}_{\mathrm{opt}}^*\right)=1.\end{aligned} \tag{28}$$

Likewise, $rank(\mathbf{Z}_{1,\mathrm{opt}})=0$ cannot appear because the equality constraint in problem (23) needs to be satisfied.

Theorem 2 shows that problem (23) is indeed equivalent to problem (21). Meanwhile, the optimal solution $\mathbf{z}_{1,\mathrm{opt}}$ of problem (21) can be obtained by $\mathbf{z}_{1,\mathrm{opt}}=\mathrm{P}(\mathbf{Z}_{1,\mathrm{opt}}/\eta_{\mathrm{opt}})$, $\Sigma_{\mathrm{opt}}=\mathbf{X}_{\mathrm{opt}}/\eta_{\mathrm{opt}}$. Among them, $\mathrm{P}(\cdot)$ represents the operation of taking the corresponding eigenvector.

For any given τ, the inner layer problem has been optimally solved. To this end, we next turn our attention to the outer optimization problem. It can be seen that it is a univariate optimization problem.

$$\begin{aligned}&\min_\tau\frac{\Phi(\tau)}{1+\tau\gamma_{D,\mathrm{opt}}^{(2)}\Phi(\tau)}\\ &\text{s.t.}\tau_{\mathrm{lb}}\le\tau\le\tau_{\mathrm{ub}}.\end{aligned} \tag{29}$$

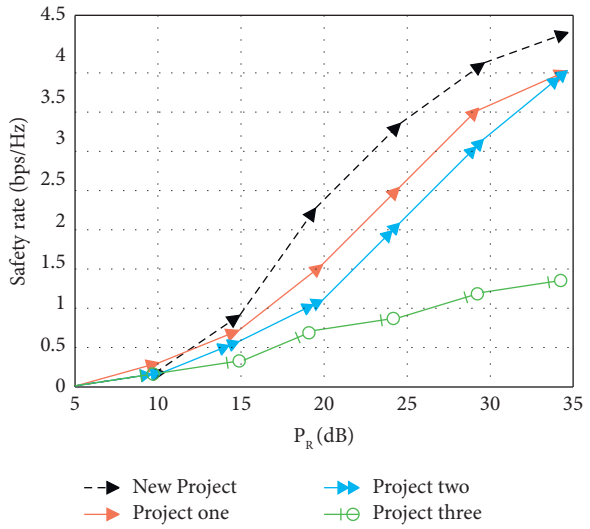

Figure 3: Curve of safe rate versus total relay power budget P_R, $K_R = 5, K_J = 10, M = 3, P_S = 20\text{dB}, P_{1,i} = P_{2,k} = P_D = P_R/(K_J + K_R)$.

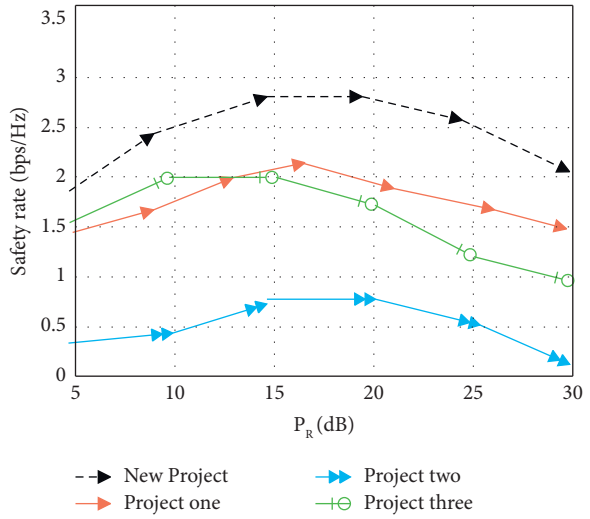

Figure 4: The curve of the safe rate with respect to the transmit power P_S of the source $K_R = 5, K_J = 10, M = 3, P_R = 25\text{dB}$, $P_{1,i} = P_{2,k} = P_D = P_R/(K_J + K_R)$.

In the formula, τ_{lb} and τ_{ub} represent the lower and upper bounds of $\log(1 + \gamma_{E,l}^{(1)}) \le \log(1/\tau), \forall l$ implied in the constraint τ, respectively. $\tau \le 1 \triangleq \tau_{\text{ub}}$ can be obtained by carefully observing the feasibility of this constraint. Furthermore, an effective $\tau_{\text{lb}}\,(>0)$ is derived from the following relation:

$$\gamma_{E,l} = \frac{P_S\left|\mathbf{h}_{0,l}\right|^2}{\text{Tr}\left(\mathbf{H}_l\boldsymbol{\Sigma}\right) + 1} < \frac{1}{\tau} - 1 < \max_l\left(P_S\left|\mathbf{h}_{0,l}\right|^2\right). \tag{30}$$

The expression about the lower bound can be obtained by sorting the following:

$$\tau \ge \frac{1}{\left(1 + \max_l P_S\left|\mathbf{h}_{0,l}\right|^2\right)} \triangleq \tau_{\text{lb}}. \tag{31}$$

Because problem (31) is a univariate optimization problem on a finite interval with interval lengths less than 1,

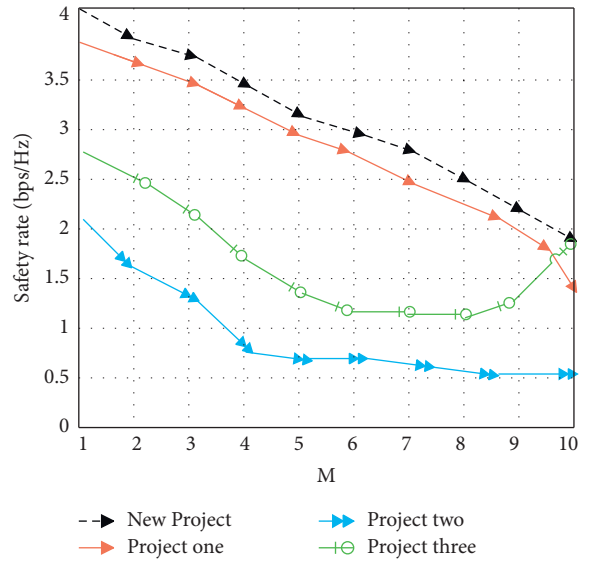

Figure 5: The curve of the security rate with respect to the number M of eavesdropping nodes.

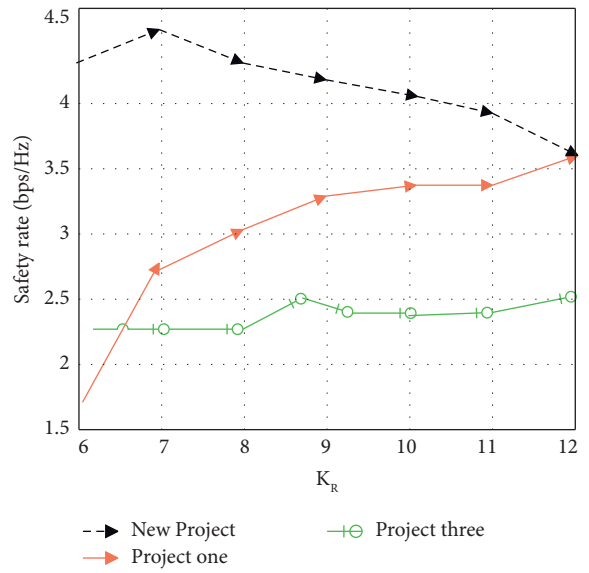

Figure 6: The curve of the safe rate with respect to the number of cooperative relays K_R and the number of interfering relays K_J allocation scheme.

many one-dimensional optimization techniques that require no derivatives can be used to search for an optimal solution to problem (31). In practice, in order to reduce the complexity, the golden-section search can be used, which guarantees that at least one local optimal solution can be found.

This section presents some simulation results to verify the safe rate performance of the proposed transmission strategy. Because the distance between the cooperative relay and the interfering relay is relatively short, it is assumed that the channel between them obeys the complex Gaussian distribution of $\mathbf{G} \sim \text{CN}(0, 10\mathbf{I}_{K_J})$, and the rest of the channels obey the standard complex Gaussian distribution $\text{CN}(0, 1)$. In the simulation, the average transmit power of

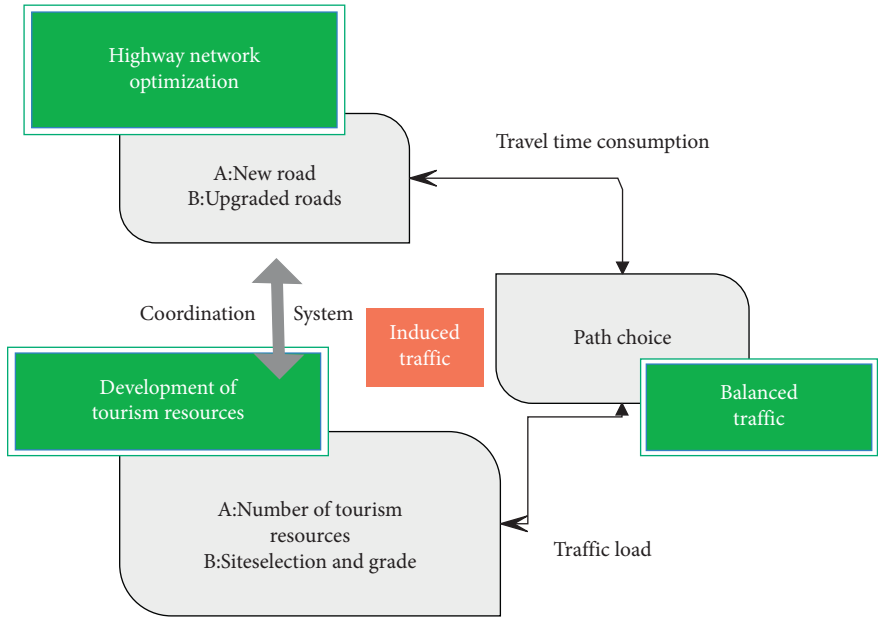

Figure 7: The game relationship between planning decision-makers and traffic travelers.

the source is set to $P_S = 20\text{dB}, P_R$, which represents the total power budget of the cooperative and interfering relays. As a comparison, we also simulate three existing traditional two-slot-based secure transmission schemes. In the first strategy, all K_J jamming relays only transmit artificial noise to jam eavesdropping nodes. In the second strategy, all relays (including K_R cooperative relays and K_J interfering relays) use the null-space design to help forward confidential signals to destination nodes. In the third strategy, the operation of the relay node is the same as the second strategy. The difference is that the destination node will act as an interfering node in the broadcast phase, and the interference is transmitted to weaken the received signal quality at the eavesdropping node.

Figure 3 presents the curves of the safe rate versus the total power budget P_R for the proposed scheme and the other three schemes. The specific parameters are that each cooperative relay and the interfering relay have the same power budget, which is $P_{1,i} = P_{2,k} = P_R/(K_J + K_R)$. The number of cooperative relays is $K_R = 5$, the number of interfering relays is $K_J = 10$, and the number of eavesdropping nodes is $M = 3$. Obviously, the proposed scheme shows the optimal safe rate performance at each power value. In addition, it can be seen from the figure that the second scheme will tend to a fixed value after the power continues to increase. This is because this transmission scheme does not protect the information leakage in the broadcast stage; the security rate will gradually reach a bottleneck.

Figure 4 plots the safe rate curves of different schemes with respect to the source transmit power P_S when there is $K_R = 5, K_J = 10, M = 3, P_R = 25\text{dB}$. As can be seen, the proposed transmission strategy exhibits the best performance. Moreover, with the increase in the transmit power of the source, the security rate will experience a process of first increasing and then decreasing. This is because when P_S is relatively small, the source transmit power is increased, which can significantly improve the received signal-to-noise ratio of the destination node. When P_S is larger, the information leakage of the first time slot will become more serious.

Figure 5 illustrates the relationship between the security rate and the number M of eavesdropping nodes. In this simulation, $P_R = 20\,\text{dB}, K_R = 10, K_J = 20$ is set. We note that in the proposed scheme, the selection of M needs to satisfy the $M < \min\{K_R, K_J - K_R\} = 10$ constraint to ensure that there are enough spatial degrees of freedom to design the beamforming weight vector. First, it can be seen that the proposed scheme exhibits obvious advantages when the number of eavesdropping nodes is much smaller than the number of cooperative relays and interfering relays. When the number of eavesdropping nodes gradually increases, the security rate of all schemes decreases. Within the limited value range of M, the proposed scheme still shows the best performance.

Figure 6 considers the scenario of $K = 30, M = 5, P_S = 20\text{dB}$, $P_R = 25\text{dB}$, and shows the curve of the safe rate and the value of cooperative relay K_R. Since there is $M = 5$, in order to ensure enough degrees of freedom in space, K_R can take all the possibilities of the abscissa in the figure. As can be seen from the curve of scheme 3, since it assumes that all relays are used as cooperative relays, the allocation of the number of K_R and K_J does not affect its safe speed.

However, for the proposed scheme and scheme 1, how to allocate the number of cooperative relays and interfering relays has an impact on the security rate. As can be seen from the figure, after the number of cooperative relays increases in scheme 1, the security rate has a significant improvement. Moreover, the proposed scheme is relatively stable over the entire range of possible values, with only a small downward trend. This shows that the proposed scheme does not need to think too much about how to distribute the relays. In addition, there is still a gap of about 0.6 bps/Hz between the

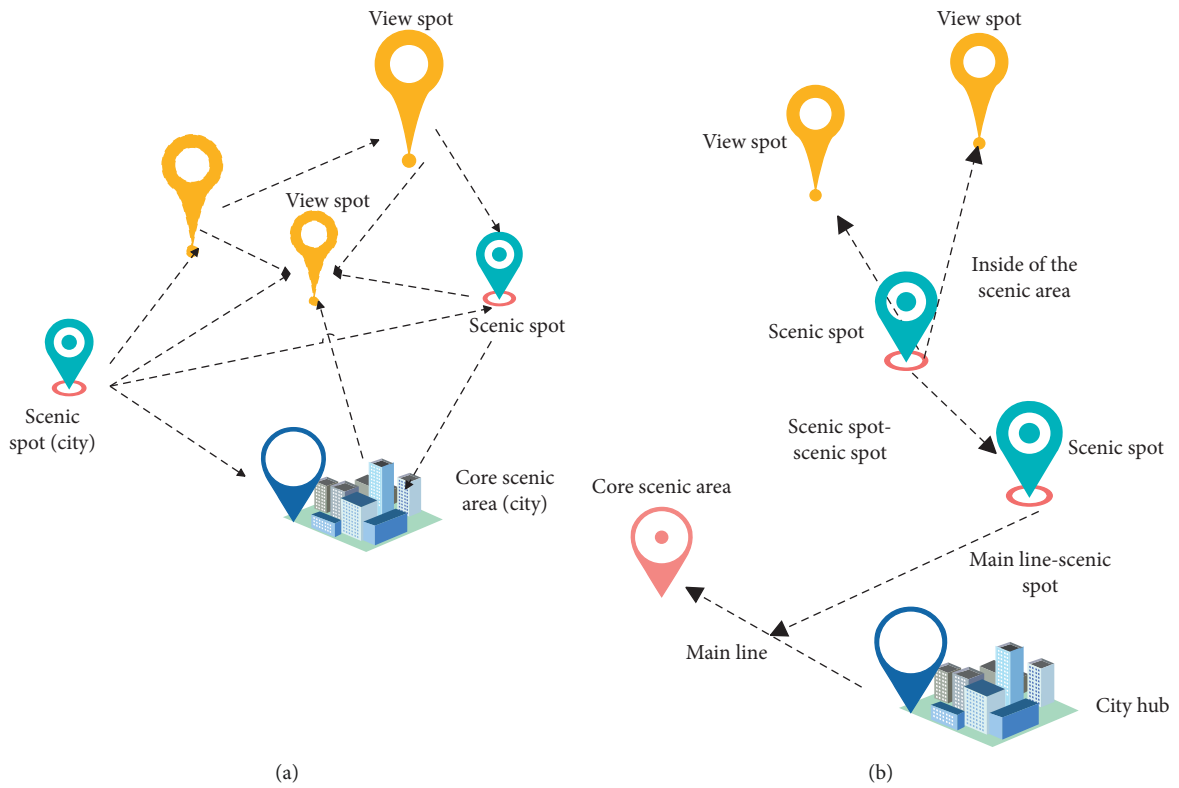

Figure 8: Schematic diagram of tourism and road network, (a) desired itinerary for tourist trips, and (b)schematic diagram of functional classification of tourist roads.

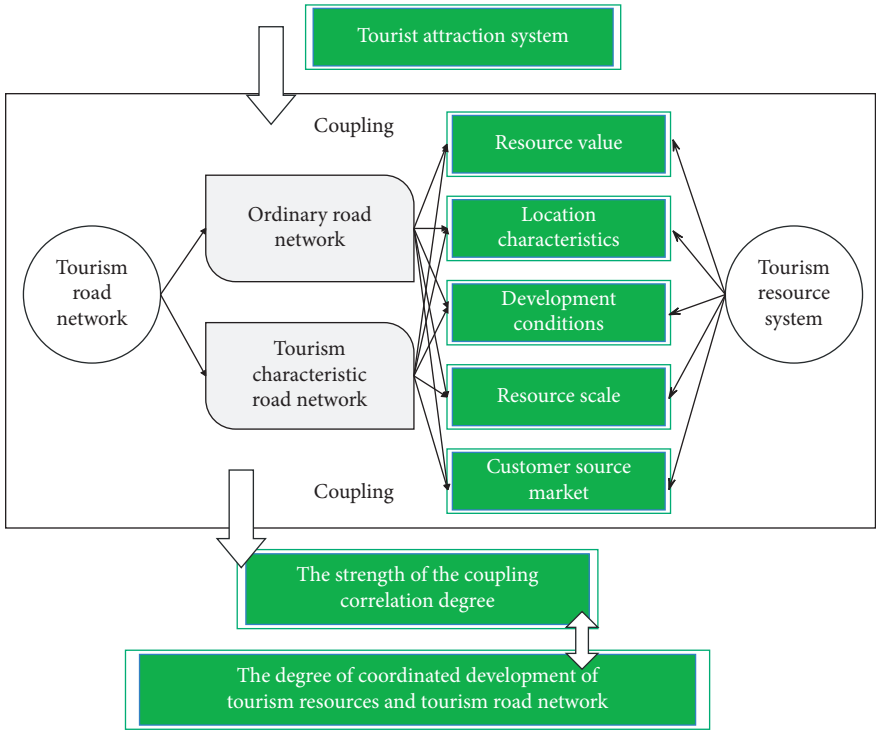

Figure 9: The coupling between the tourism road network and the tourism resource complex system.

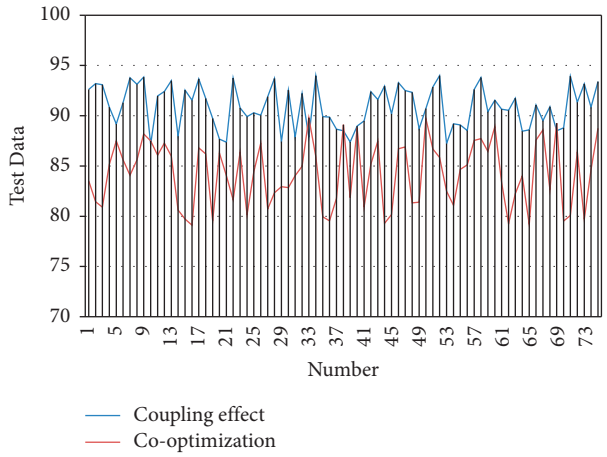

Figure 10: Coupling effect and optimization effect of the collaborative optimization model of tourism resources and highway network based on deep learning.

optimal performance point of scheme 1 and the optimal performance point of the proposed scheme.

4. Model Building

During the process of tourism resource development and road network construction, the travel (including tourists) will be affected. The game relationship between traffic travelers and planners is shown in Figure 7.

Generally speaking, road tourism is a process in which tourists travel from the tourist source to the tourist destination and back through the road. In this paper, tourism resources are used as the nodes of the road network, which mainly include cities, core scenic spots, and scenic spots and scenic spots. It is necessary to break the circle or add edges to the tourist road network, and establish a reasonable and effective tourist road network with complete functions, as shown in Figure 8(b). Corresponding tourist highway functions are classified as follows: urban hub-scenic area road (including the main line of tourism service and main line-scenic area tourist road), scenic area-scenic area tourist road, and scenic spot (scenic spot-scenic spot) tourist road.

This paper analyzes the mechanism of the coupling system between tourist roads and resources. Moreover, on the basis of constructing the evaluation index system of the spatial coupling between the tourist road network and the tourist resources, this paper adopts the gray relational analysis method to quantitatively reveal the main factors and the degree of coupling correlation between the tourism road network and the tourism resource space from the perspective of time and space, so as to show the scientificity and rationality of the tourism road network layout planning based on the perspective of tourism resources. The coupling between the tourism road network and the tourism resource composite system is shown in Figure 9.

The coupling effect and optimization effect of the collaborative optimization model of tourism resources and highway network based on deep learning proposed in this paper are verified, and the experimental analysis is carried out in combination with the actual situation. The statistical simulation test results are shown in Figure 10.

From the above research, it can be seen that the collaborative optimization model of tourism resources and highway network based on deep learning proposed in this paper can effectively promote the collaborative optimization of tourism resources and highway network.

5. Conclusions

The vigorous development of the economy has brought about the continuous improvement of people's living standards. People's demand for tourism activities is also showing a blowout development, whether it is a suburban trip or a long-distance trip, and even the number of foreign trips is increasing year by year. However, the premise of travel is that it needs good transportation facilities to support it. For this reason, the country is constantly improving the construction of infrastructure, especially the construction of transportation, and the annual increase in high-speed mileage ranks first in the world. While vigorously supporting the tourism industry, the country is also insisting on expanding its opening to the outside world, strengthening international economic cooperation, and creating new opportunities for the better development of the tourism industry. At this stage, the development of tourism has gradually transformed from the early single-point breakthrough and advanced development model to the development model of regional cooperation and system integration. Making development and optimization plans from the perspective of a single system can easily lead to repeated infrastructure configuration, and it is difficult to improve the level of resource utilization. Therefore, from the perspective of system coordination, it is necessary to realize the reconfiguration and combination of resources through the integration of the tourism system and the highway transportation system, so as to maximize the regional economic benefits. This paper combines deep learning algorithms to build a collaborative optimization model of tourism resources and highway network, verifies the dependence of tourism travel on the transportation network, and determines the potential development points of tourism resources in the network and the optimization and improvement points of the road network, so as to coordinate the tourism resources and the highway network. Optimization provides a reliable basis. The research shows that the collaborative optimization model of tourism resources and highway network based on deep learning proposed in this paper can effectively promote the collaborative optimization of tourism resources and highway network. In actual life, it can facilitate people's travel, improve the convenience and comfort of tourism, accelerate the mining and promotion of local tourism resources, and drive the local economy to develop along with the green management model.

Data Availability

The labeled datasets used to support the findings of this study are available from the corresponding author upon request.

Conflicts of Interest

The authors declare no conflicts of interest.

Acknowledgments

The research was supported by the "Blue Project" involving Universities and Colleges of Jiangsu Province in 2021.

References

[1] K. Nam, C. S. Dutt, P. Chathoth, and M. S. Khan, "Blockchain technology for smart city and smart tourism: latest trends and challenges," *Asia Pacific Journal of Tourism Research*, vol. 26, no. 4, pp. 454–468, 2021.

[2] C. D. Huang, J. Goo, K. Nam, and C. W. Yoo, "Smart tourism technologies in travel planning: the role of exploration and exploitation," *Information & Management*, vol. 54, no. 6, pp. 757–770, 2017.

[3] T. Brandt, J. Bendler, and D. Neumann, "Social media analytics and value creation in urban smart tourism ecosystems," *Information & Management*, vol. 54, no. 6, pp. 703–713, 2017.

[4] A. K. Tripathy, P. K. Tripathy, N. K. Ray, and S. P. Mohanty, "iTour: the future of smart tourism: an IoT framework for the independent mobility of tourists in smart cities," *IEEE consumer electronics magazine*, vol. 7, no. 3, pp. 32–37, 2018.

[5] E. Sigalat-Signes, R. Calvo-Palomares, B. Roig-Merino, and I Garcia-Adan, "Transition towards a tourist innovation model: the smart tourism destination," *Journal of Innovation & Knowledge*, vol. 5, no. 2, pp. 96–104, 2020.

[6] H. Lee, J. Lee, N. Chung, and C. Koo, "Tourists' happiness: are there smart tourism technology effects?" *Asia Pacific Journal of Tourism Research*, vol. 23, no. 5, pp. 486–501, 2018.

[7] C. Koo, L. Mendes-Filho, and D. Buhalis, "Smart tourism and competitive advantage for stakeholders: guest editorial[J]," *Tourism Review*, vol. 74, no. 1, pp. 1–4, 2019.

[8] T. Zhang, C. Cheung, and R. Law, "Functionality evaluation for destination marketing websites in smart tourism cities," *Journal of China Tourism Research*, vol. 14, no. 3, pp. 263–278, 2018.

[9] M. A. C. Ruíz, S. T. Bohorquez, and J. I. R. Molano, "Colombian tourism: proposal app to foster smart tourism in the country," *Advanced Science Letters*, vol. 23, no. 11, pp. 10533–10537, 2017.

[10] W. Wang, N. Kumar, J. Chen et al., "Realizing the potential of the internet of things for smart tourism with 5G and AI," *IEEE Network*, vol. 34, no. 6, pp. 295–301, 2020.

[11] I. Guerra, F. Borges, J. Padrão, J. Tavares, and M. Padrao, "Smart cities, smart tourism? The case of the city of Porto," *Revista Galega de Economia*, vol. 26, no. 2, pp. 129–142, 2017.

[12] Y. Topsakal, M. Bahar, and N. Yüzbaşioğlu, "Review of smart tourism literature by bibliometric and visualization analysis," *Journal of Tourism Intelligence and Smartness*, vol. 3, no. 1, pp. 1–15, 2020.

[13] S. Joshi, "Social network analysis in smart tourism driven service distribution channels: evidence from tourism supply chain of Uttarakhand, India," *International Journal of Digital Culture and Electronic Tourism*, vol. 2, no. 4, pp. 255–272, 2018.

[14] F. Femenia-Serra, B. Neuhofer, and J. A. Ivars-Baidal, "Towards a conceptualisation of smart tourists and their role within the smart destination scenario," *Service Industries Journal*, vol. 39, no. 2, pp. 109–133, 2019.

[15] C. Koo, F. Ricci, C. Cobanoglu, and F Okumus, "Special issue on smart, connected hospitality and tourism," *Information Systems Frontiers*, vol. 19, no. 4, pp. 699–703, 2017.

[16] H. Abdel Rady and A. Khalf, "Towards smart tourism destination: an empirical study on sharm el sheikh city, Egypt," *International Journal of Heritage, Tourism and Hospitality*, vol. 13, no. 1, pp. 78–95, 2019.

[17] T. Pencarelli, "The digital revolution in the travel and tourism industry," *Information Technology & Tourism*, vol. 22, no. 3, pp. 455–476, 2020.

[18] C. J. P. Abad and J. F. Álvarez, "Landscape as digital content and a smart tourism resource in the mining area of cartagena-La unión (Spain)," *Land*, vol. 9, no. 4, pp. 1–22, 2020.